ELSEVIER

Biophysical Chemistry 96 (2002) 293–303

Biophysical Chemistry

www.elsevier.com/locate/bpc

Folding and intrinsic stability of deletion variants of PrP(121–231), the folded C-terminal domain of the prion protein

Heike Eberl, Rudi Glockshuber*

Institut für Molekularbiologie und Biophysik, Eidgenössische Technische Hochschule Hönggerberg, CH-8093 Zürich, Switzerland

Received 26 October 2001; received in revised form 5 November 2001; accepted 12 November 2001

Abstract

Transmissible spongiform encephalopathies in mammals are believed to be caused by PrP^{Sc}, the insoluble, oligomeric isoform of the cellular prion protein PrP^{C}. PrP^{C} and the subunits of PrP^{Sc} have identical covalent but different tertiary structure. To address the question of whether parts of the structure of PrP^{C} are sufficiently stable to be retained in PrP^{Sc}, we have constructed two deletion variants of the C-terminal PrP^{C} domain, PrP(121–231), which is the only part of recombinant PrP with defined tertiary structure. One of the variants, H2–H3, comprises the last two α-helices of PrP(121–231) that have been proposed to be preserved in models of PrP^{Sc}. In the other variant, PrP(121–231)-ΔH1, the first α-helix of PrP(121–231) was deleted and replaced by introduction of the β-turn dipeptide Asn–Gly between the strands of the single β-sheet of PrP(121–231). Although both deletion constructs still show α-helical CD-spectra, they are more disordered and thermodynamically strongly destabilized compared to PrP(121–231), with free energies of folding close to zero. These data demonstrate that the tertiary structure context is critical for the conformation of the segment comprising α-helix 2 and 3 in the solution structure of recombinant PrP.

Keywords: Prion protein; Deletion variants; Stability; Structure of PrP^{Sc}

Abbreviations: CD, circular dichroism; CJD, Creutzfeldt–Jakob disease; FFI, fatal familial insomnia; GdmCl, guanidinium chloride; GSS, Gerstmann–Sträussler–Scheincker syndrome; H2–H3, segment of PrP comprising residues 170–231, corresponding to α-helices 2 and 3; MALDI-TOF, matrix-assisted laser desorption time-of-flight mass spectrometry; PrP^{C}, cellular prion protein; PrP^{Sc}, scrapie isoform of the prion protein; PrP(121–231), folded C-terminal domain of recombinant PrP; PrP(121–231)-ΔH1, deletion variant of PrP(121–231) lacking α-helix 1 (residues 135–160 are replaced by the β-turn dipeptide Asn–Gly); MES, morpholinoethane–sulfonic acid; Tris, Tris–hydroxymethyl-aminomethane; TSE, transmissible spongiform encephalopathy

*Corresponding author. Tel.: +41-1633-6819; fax: +41-1633-1036.

E-mail address: rudi@mol.biol.ethz.ch (R. Glockshuber).

0301-4622/02/$ - see front matter
PII: S0301-4622(02)00015-7

1. Introduction

The 'protein-only' hypothesis states that transmissible spongiform encephalopathies (TSEs) in mammals such as the human Creutzfeldt–Jakob disease (CJD) and bovine spongiform encephalopathy (BSE) in cattle, are caused by propagation of PrP^{Sc}, the abnormal oligomeric isoform of the cellular prion protein (PrP^{C}) of the host [1,30,31,33,47]. Although the 'protein-only' hypothesis is still not entirely proven for mammalian TSEs, there are strong arguments supporting a protein-based prion propagation mechanism. In particular, these are the findings that mice devoid of PrP are resistant to prions [4], that less than one molecule nucleic acid of >100 bps could be detected per infectious unit in enriched prion preparations [15,16], that prions are resistant against strong UV irradiation [1,2] and that all known inherited forms of human prion diseases, i.e. inherited CJD, the Gerstmann–Sträussler–Scheincker syndrome (GSS) and fatal familial insomnia (FFI), are associated with mutations in the gene encoding human PrP [32].

Mammalian PrP^{C} is an extremely well conserved cell surface protein of unknown function consisting of approximately 210 amino acids (residues 23–231; amino acid numbering according to human PrP). Pairs of mammalian PrP sequences are generally more than 90% identical [37,49]. PrP^{C} has two N-glycosylation sites at Asn181 and Asn197, a glycosyl-phosphatidyl-inositol (GPI) anchor at its C-terminal residue 231, and a single disulfide bond between Cys179 and Cys214 [41]. PrP^{C} is a monomeric protein, soluble in non-denaturing detergents, and shows α-helical circular dichroism (CD) and infrared spectra. In contrast, PrP^{Sc} is an ordered oligomer with a protease-resistant core comprising residues 90–231 [3,29,25], and the PrP^{Sc} subunits show an increased β-sheet and a lower α-helix content compared to PrP^{C}.

Although the molecular mechanism underlying the formation of PrP^{Sc} from PrP^{C} is unknown, it has become clear that PrP^{Sc} and PrP^{C} have identical covalent structures [41,42] and differ exclusively in their tertiary structures and association states. Consequently, knowledge of the three-dimensional structures of PrP^{C} and PrP^{Sc}, and of the folding and stability of PrP^{C}, are essential prerequisites for understanding the conversion mechanism to PrP^{Sc}. Within the last few years, the three-dimensional structures of the recombinant prion proteins from mouse [34,35], hamster [14], man [52] and cattle [23] have been determined in solution by nuclear magnetic resonance (NMR) spectroscopy. All prion protein structures are very similar with a long, flexibly disordered N-terminal region (residues 23–120) and a folded C-terminal domain, PrP(121–231) that contains three α-helices and a two-stranded, antiparallel β-sheet (Fig. 1a). Although the recombinant prion proteins were produced in bacteria and thus lack the post-translational modifications of natural PrP, they have the same biophysical properties as PrP^{C}. It is therefore generally accepted that the three-dimensional structures of recombinant PrPs are very similar or identical to the corresponding natural cellular prion proteins.

Comparison of the structures of the folded C-terminal domains of prion proteins from different species revealed a striking correlation between local differences in tertiary structure and the observed species barrier of prion transmission [5,23,52]. Specifically, the recombinant human prion protein is most similar to recombinant bovine PrP, indicating that structural similarities at the level of PrP^{C} may be involved in the generation of human new variant CJD (nvCJD), caused by transmission of BSE from cattle to humans [21,38]. In this context, one of the most important questions is whether the structure of the C-terminal domain of PrP^{C} or at least certain parts of its tertiary structure are retained in the subunits of PrP^{Sc}. Regarding the fact that segment 90–231 forms the protease resistant core of PrP^{Sc} and that PrP^{Sc} has a higher β-sheet content compared to PrP^{C}, the minimum structural rearrangement during PrP^{Sc} formation appears to be the formation of β-sheet structure in segment 90–120, preserving it from proteolytic attack after oligomerization. The other extreme would be a completely different tertiary structure of segment 121–231 in the subunits of the PrP^{Sc} oligomer. Intermediate models for the PrP^{Sc} structure have also been considered. One theoretical model predicts that the C-terminal two α-helices of PrP^{C} (helix 2 and 3),

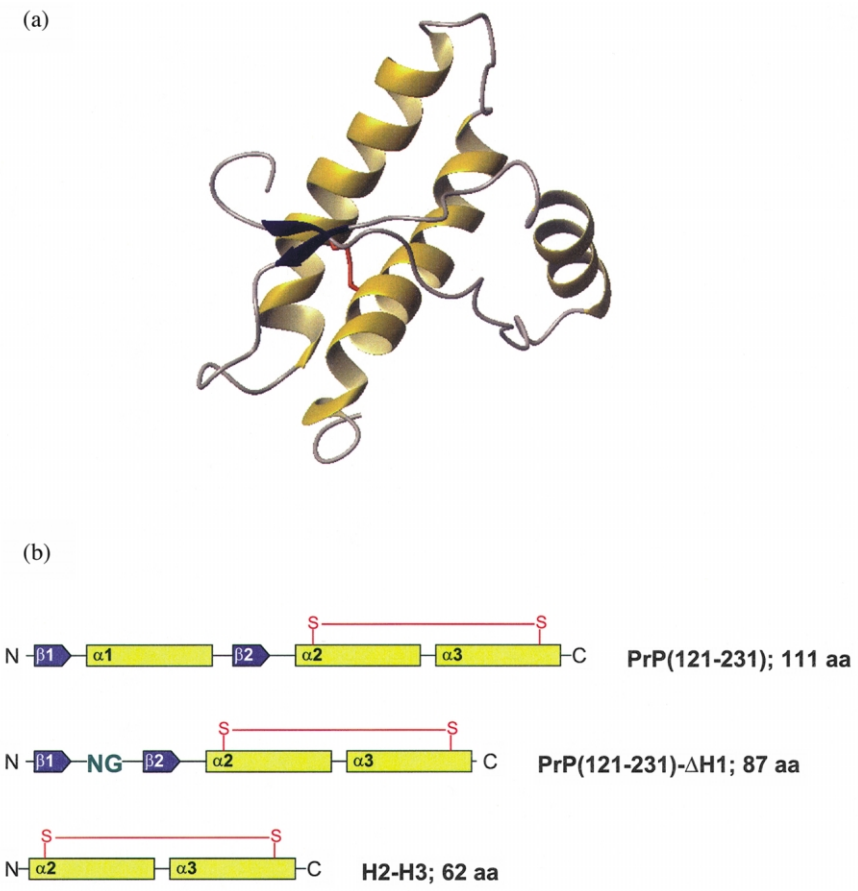

Fig. 1. Ribbon representation of murine PrP(121–231) (a) (pdb accession code, 1ag2) and linear representations of PrP(121–231) and the deletion variants PrP(121–231)-ΔH1 and H2–H3 (b). The α-helices are shown in yellow, the strands of the short β-sheet are depicted in blue. The disulfide bond Cys179–Cys214 is indicated in red, the β-turn dipeptide Asn–Gly introduced in PrP(121–231)-ΔH1 is shown in green. The figure in (a) was generated with the program MOLMOL [17].

which are connected by a disulfide bond, are still present in PrP^{Sc} subunits [12]. Alternatively, the small β-sheet in PrP^{Sc} has been proposed as a potential nucleation site for growth of the β-sheet which may, for example involve rearrangement of the segment between the two β-strands containing the rather isolated first α-helix [34,18].

In the present study, we have addressed the question of whether parts of the folded domain of murine PrP are sufficiently stable so that their structure might be retained in PrP^{Sc} subunits. For this purpose, we have generated a PrP fragment termed H2–H3 corresponding to the disulfide-linked α-helices 2 and 3 (Fig. 1b). These helices form the scaffold of the tertiary structure of recombinant PrP(121–231). In addition, we have produced a PrP(121–231) deletion variant termed PrP(121–231)-ΔH1. In this construct, the entire segment 135–160 between the two β-strands, including α-helix 1, was replaced by the β-turn sequence Asn–Gly [39,40] (Fig. 1b). Here we report that both deletion constructs partially retain α-helical structure and are thermodynamically strongly destabilized compared to the intact C-terminal domain PrP(121–231), indicating that the tertiary structure context is crucial for the conformation of the disulfide-bonded helix pair H2–H3 in recombinant PrP.

2. Materials and methods

2.1. Construction of expression plasmids for the fragments H2–H3 and PrP(121–231)-ΔH1

2.1.1. H2–H3

The gene corresponding to residues 170–231 of the mouse prion protein was amplified by the polymerase chain reaction (PCR) from the expression plasmid pPRP-CRR [9], using the two overlapping N-terminal primers N1 (5′-CATCATGGTTTAGTGCCGCGTGGGAGCAAT-CAGAACAACTTCGTG-3′) and N2 (5′-TTTT-TTTCGCGAGTCATCATCATCATCATCATGGT-TTAGTTCCG-3′), and the C-terminal primer C1 (5′-AGGAGGGGAGGGGATCCAAGCTTACTA-GCTGGAACGACGCCCGTCGTAATAG-3′). In a two-step PCR reaction with a 15-fold excess of primer N2 over N1, an N-terminal $(His)_6$-tag and a thrombin cleavage site (HHHHHHGLVPR↓GS) were introduced at the N-terminus of the H2–H3 sequence for purification with metal chelate affinity chromatography. The resulting PCR-product was digested with NruI and BamHI and cloned into the secretory T7 expression plasmid pRBI-PDI-T7 [43] behind the OmpA signal sequence via the StuI and BamHI restriction sites.

2.1.2. PrP(121–231)-ΔH1

The segment 135–160, corresponding to helix 1 of the mouse prion protein, was deleted and replaced by codons for the dipeptide Asn–Gly via Kunkel mutagenesis [19,20] using uridinylated single-stranded DNA of pPRP-CRR [46], and the mutagenesis primer 5′-TGATCCACCGGGCGGT-AGTATACTTGGTTGCCGTTCATGGCGCTCC-CCAGCATGTAGCCACCCAG-3′. The resulting plasmid was then used as template for introduction of the N-terminal $(His)_6$-tag and thrombin cleavage site and cloning into pRBI-PDI-T7 as described above, except that primer N3 (5′-CA-TCATGGTTTGGTTCCGCGTGGGAGTGTAGT-GGGTGGCCTTGG-3′) was used instead of N1. Both constructs were verified by dideoxynucleotide sequencing of the complete genetic sequences of the PrP constructs.

2.2. Expression and purification of PrP(121–231)-ΔH1 and H2–H3

The constructs H2–H3 and PrP(121–231)-ΔH1 were expressed and purified according to the following procedure: cells of *E. coli* BL21(DE3) harboring either expression plasmid were grown at 37 °C in 10 l of LB medium containing ampicillin (100 μg/l). At an optical density (OD) at 550 nm of 1.2, protein expression was induced by addition of IPTG to a final concentration of 1 mM. Cell growth was continued at 37 °C for 6 h and the cells were harvested by centrifugation. Cells were resuspended in 50 mM Tris/HCl pH 8.0, 1 mM $MgCl_2$, 4 mg/ml DNase I, 4 mg/ml RNase A, 10 mg/ml lysozyme) and disrupted in a French Pressure Cell (18 000 psi, SLM Aminco). H2–H3 and PrP(121–231)-ΔH1, were obtained as periplasmic inclusion bodies and found in the insoluble fraction after lysis and centrifugation (30 min, 49 000 g and 4 °C). The inclusion bodies were resuspended in buffer A (6 M GdmCl, 20 mM Tris/HCl of pH 8.0, and 100 mM sodium phosphate), and applied to an Ni-NTA column (Qiagen, Basel, Switzerland) equilibrated with the same buffer. Proteins were refolded on the column by a linear gradient from buffer A to buffer B (20 mM Tris/HCl pH 8.0, 100 mM sodium phosphate) and were eluted with 1 M imidazole/HCl in buffer B.

Eluted proteins were then dialyzed against 10 mM Tris/HCl pH 8.5, and the $(His)_6$-tag was cleaved off by digestion with thrombin (0.1 U/ml) for 2 h at 22 °C. Further purification—in particular separation of uncleaved protein—was carried out on a Superdex 75 (Amersham–Pharmacia, Dübendorf, Switzerland) gel filtration column in 20 mM Tris/HCl of pH 8.5, and 1 mM EDTA. Fractions containing pure protein were combined, dialyzed against 5 mM Tris/HCl, pH 8.5, concentrated and stored at −20 °C. Yields were approximately 0.5 mg of pure protein per liter of LB medium for both constructs.

Ellman assays [6] showed that the single disulfide bridge in both constructs was formed quantitatively. Edman sequencing demonstrated complete cleavage of the N-terminal $(His)_6$-Tag. This was also confirmed by MALDI-TOF mass spectrometry [PrP(121–231)-ΔH1, calculated mass = 10 386

Da and measured = 10 389 Da; H2–H3, calculated mass = 7408 Da and measured = 7405 Da). Analytical gel filtration of the constructs on a Superdex 75 column in 20 mM Tris/HCl pH 8.5, 1 mM EDTA demonstrated that both H2–H3 and PrP(121–231)-ΔH1 were eluted as monomers.

Expression and purification of murine PrP(121–231) and PrP(23–231) was carried out as described previously [22].

2.3. Protein concentrations

Protein concentrations were determined by absorbance spectroscopy using the specific absorbances ($A_{280\ nm,\ 1\ mg/ml,\ 1\ cm}$) determined according to [7]: 0.61 for H2–H3; 1.00 for PrP(121–231)-ΔH1; 1.55 for PrP(121–231); and 2.70 for PrP(23–231).

2.4. Far-UV-CD spectra

Far-UV-CD spectra were measured at 22 °C on a Jasco 710 CD spectropolarimeter in 0.1-cm quartz cuvettes, accumulated 15 times and corrected for buffers. Protein samples containing 15 μM of the respective protein were centrifuged (30 min, 21 000 × *g*, 4 °C) prior to concentration determination and CD measurements in order to remove possible aggregates.

Between pH 3.0 and 8.0, the following buffers were used: pH 3.0, 50 mM formic acid/NaOH, 24 mM NaCl; pH 4.0, 50 mM formic acid/NaOH; pH 5.0, 50 mM acetic acid/NaOH, 56 mM NaCl; pH 6.0, 10 mM MES/NaOH, 84 mM NaCl; pH 7.0, 50 mM NaH_2PO_4/NaOH; and pH 8.0, 50 mM Tris/HCl, 56 mM NaCl. A constant ionic strength of 88 mM was maintained between pH 5.0 and 8.0. At pH values below 5.0, the ionic strength had to be reduced to 34 mM due to aggregation of H2–H3- and PrP(121–231)-ΔH1 at higher ionic strengths above this value.

2.5. Urea-induced equilibrium transitions

Reversible unfolding and refolding of H2–H3, PrP(121–231)-ΔH1 and PrP(121–231) was measured at 22 °C at pH 4.0 and 7.0 in the buffers mentioned above, containing different concentrations of urea. For refolding experiments, the respective proteins were first denatured in 8 M urea for 1 h at room temperature. Stock solutions of native or denatured protein were then diluted 1:11 with buffer to a final protein concentration of 15 μM.

After 24 h of incubation the equilibrium transitions were monitored at 222 nm and 22 °C on a Jasco 710 CD spectropolarimeter in 0.1-cm quartz cuvettes. The averaged ellipticities were corrected for buffer, and urea concentrations were determined by refractometry. The transitions were evaluated according to a two-state equilibrium with a six-parameter fit [36].

2.6. Disulfide bond reduction

Reduction of either H2–H3 or PrP(121–231)-ΔH1 was achieved under denaturing conditions by incubating the proteins for 2 h at room temperature in 8 M urea, 50 mM Tris/HCl pH 8.0, 50 mM DTT, and 1 mM EDTA. The protein samples were then dialyzed against 50 mM formic acid/NaOH pH 4.0, 1 mM EDTA and far-UV-CD spectra of the reduced proteins were recorded as described above. Complete reduction was confirmed by Ellman assays [6].

3. Results and discussion

3.1. Expression, refolding and purification of PrP(121–231)-ΔH1 and H2–H3

In contrast to the isolated C-terminal domain of murine PrP, PrP(121–231) [9], the truncated domain variants PrP(121–231)-ΔH1 and H2–H3 could not be produced as soluble proteins in the periplasm of *E. coli* using the OmpA signal sequence. Both proteins were correctly processed, but accumulated in periplasmic inclusion bodies. This already indicated a lower stability of the deletion constructs compared to the wild type domain, as periplasmically expressed PrP(121–231) variants with reduced stability also aggregate in the periplasm while variants with unchanged stability stay soluble [22]. For convenient purification and refolding of PrP(121–231)-ΔH1 and H2–H3 from periplasmic inclusion bodies with

metal chelate affinity columns, a hexahistidine sequence followed by a thrombin recognition site was inserted between the OmpA-signal sequence and the first residues of the truncated domains (see [51] and Section 2). The tagged constructs were correctly processed by signal peptidase and also formed inclusion bodies in the periplasm. PrP(121–231)-ΔH1 and H2–H3 were solubilized with 6 M guanidinium chloride (GdmCl), refolded on the Ni-NTA columns, eluted with imidazole and purified to homogeneity by gel filtration after thrombin cleavage of the $(His)_6$-tag [51]. The homogeneity of the N-termini was verified by Edman sequencing and mass spectrometry, and Ellman assays proved complete formation of the single disulfide bond in both proteins. Both constructs could be concentrated to approximately 200 μM and, like PrP(121–231), proved to be monomeric in analytical gel filtration experiments when applied to the column at a concentration of 200 μM (data not shown).

3.2. Both PrP(121–231)-ΔH1 and H2–H3 exhibit α-helical structure between pH 3.0 and 8.0

To analyze the structural consequences of the deletions for PrP(121–231)-ΔH1 and H2–H3, far-UV-CD spectra of the deletion variants were recorded in the range of pH 3.0–8.0 and compared with those of PrP(121–231) (Fig. 2). Both PrP(121–231)-ΔH1 and H2–H3 show mainly α-helical far-UV-CD spectra with the typical minima at 208 and 222 nm, albeit the first minimum at 208 nm is slightly shifted towards lower wavelengths in both constructs relative to wild type PrP(121–231). Both deletion constructs show less negative molar mean residue ellipticities compared to PrP(121–231). Particularly in the case of the construct H2–H3, the spectral data indicate that the overall α-helix content in the deletion variant is significantly lower than in PrP(121–231), which could be confirmed by the low unfolding cooperativities observed for H2–H3 (Table 1).

Far-UV-CD spectra of the construct PrP(121–231)-ΔH1 were completely independent of pH, as was observed for wild type PrP(121–231) in the range of pH 4.0–7.0. In the case of H2–H3, the spectra at pH 4.0 exhibit more negative mean

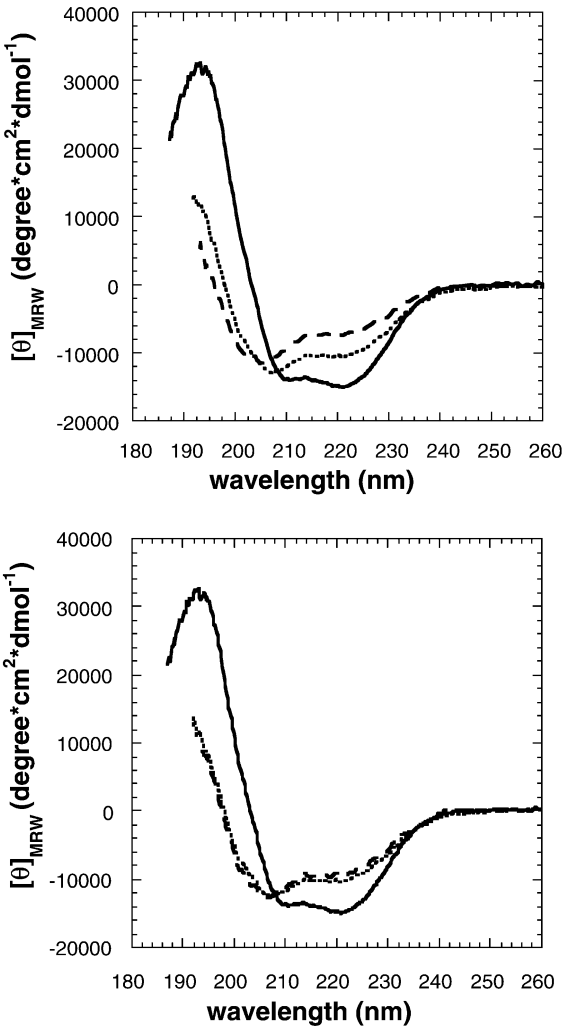

Fig. 2. Far-UV-CD spectra of PrP(121–231) (solid line), PrP(121–231)-ΔH1 (dotted line) and H2–H3 (dashed line) at pH 7.0 (a) and 4.0 (b).

residue ellipticities compared to those at neutral pH, and can be explained by a higher thermodynamic stability of the segment at acidic pH (see below) (Fig. 2b).

3.3. PrP(121–231)-ΔH1 and H2–H3 are thermodynamically strongly destabilized compared to PrP(121–231)

The thermodynamic stabilities of PrP(121–231)-ΔH1 and H2–H3 at neutral pH (7.0) were

Table 1
Thermodynamic stabilities of PrP(121–231), PrP(121–231)-ΔH1 and H2–H3 at 22 °C

	ΔG°_{fold} (kJ mol^{-1})	$\Delta\Delta G^{\circ}_{fold}$ (variant-wt)	*m*-value (kJ mol^{-1} M^{-1})	$[urea]_{1/2}$ (M)
pH 4.0, 34 mM ionic strength:				
PrP(121–231) (13.3 kDa)	−16.9±0.5	–	4.0±0.1	4.2
PrP(121–231)-ΔH1 (10.4 kDa)	−4.4±1.0	12.5±1.5	2.2±0.2	2.0
H2–H3 (7.4 kDa)	−3.1±0.3[a]	13.8±1.3	1.9±0.1	1.6
pH 7.0, 88 mM ionic strength:				
PrP(121–231) (13.3 kDa)	−30.5±1.3	–	4.8±0.2	6.3
PrP(121–231)-ΔH1 (10.4 kDa)	−7.2±0.8	23.3±2.1	2.7±0.2	2.7
H2–H3 (7.4 kDa)	−0.6±0.7[a]	29.9±1.5	1.5±0.2	0.4

[a] The slope of the pre-transition baseline was fixed to zero during fitting of the data according to a two-state model of folding [36].

determined at an ionic strength of 88 mM by urea-induced folding transitions, i.e. the same conditions used previously for characterization of folding of PrP(121–231) [10]. All transitions at pH 7.0 were fully reversible and revealed a strong destabilization of the deletion constructs compared to wild type PrP(121–231). Two-state analysis yielded very low free energies of folding of −4.4 and −3.1 kJ/mol for PrP(121–231)-ΔH1 and H2–H3, respectively (Fig. 3a, Table 1). The cooperativities of folding at pH 7.0 (*m*-values) of the deletion constructs were significantly lower than the values expected from the reduced size of the variants (87 and 62 residues for PrP(121–231)-ΔH1 and H2–H3, respectively, compared to 111 residues for PrP(121–231) [28]. This is particularly true for the construct H2–H3, which shows a more than four-fold lower cooperativity than PrP(121–231) at pH 7.0 (Table 1). This observation is, however, fully consistent with the weak α-helical CD signal of H2–H3 (Fig. 2), and demonstrates that helices 2 and 3 are not completely formed in the H2–H3 variant. In accordance, the CD signal of H2–H3 at 222 nm was shifted from −7800 to −14 000 degree·cm^2·dmol^{-1} upon addition of the α-helix inducing reagent trifluoroethanol (40% v/v) (data not shown).

Both deletion variants showed a strong tendency to aggregate at acidic pH at an ionic strength of 88 mM, but were completely soluble at lower ionic strength (34 mM). Therefore, the thermodynamic stabilities of H2–H3 and PrP(121–231)-ΔH1 were measured at low salt concentrations. Under these conditions, PrP(121–231) does not form the previously described acid-induced unfolding intermediate and, as observed at pH 7.0, shows two-state unfolding behavior (Fig. 3b) [8,10,27,44]. The transitions at pH 4.0 also revealed a strong destabilization of the deletion constructs and low *m*-values compared to PrP(121–231) (Fig. 3b, Table 1). The construct H2–H3 is slightly more stable at pH 4.0 than at pH 7.0. This agrees with its weaker α-helical CD signal at neutral pH and the fact that a considerable fraction of the molecules is unfolded at pH 7.0 in the absence of denaturant (Fig. 3a, Table 1).

3.4. PrP(121–231)-ΔH1 and H2–H3 maintain α-helical far-UV-CD spectra upon reduction

Previous experiments have shown that reduction of the single disulfide bond in recombinant PrP leads to a structural rearrangement towards β-sheet structure at acidic pH, reminiscent of PrP^{Sc}

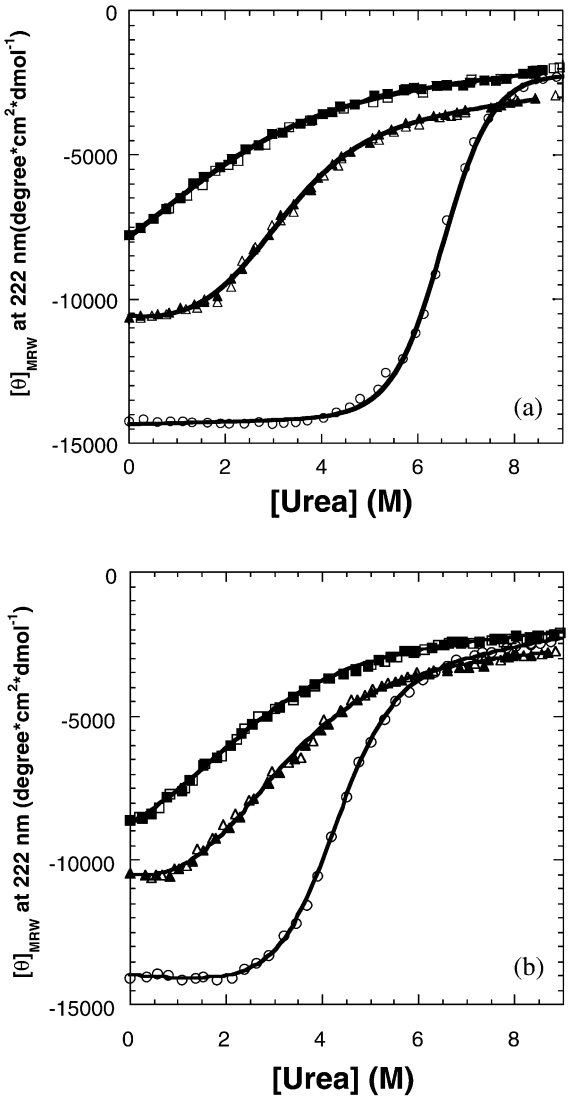

Fig. 3. Urea-induced equilibrium transitions of PrP(121–231) (molecular mass = 13.3 kDa; circles), PrP(121–231)-ΔH1 (molecular mass = 10.4 kDa; triangles) and H2–H3 (molecular mass = 7.4 kDa; squares), measured by their far-UV-CD signal of 222 nm at 22 °C and pH 7.0 (a) and 4.0 (b). Open and closed symbols represent unfolding and refolding experiments, respectively. The lines correspond to fits according to the two-state model of folding (see Table 1).

[13,24,26,50]. This led to the hypothesis that reduction or transient reduction of the disulfide bond may be involved in the mechanism of the transition of PrP^{C} to PrP^{Sc}. To test whether a transition to β-sheet structure can also be observed for the deletion variants, we recorded far-UV-CD spectra of the reduced proteins. The spectra were compared with the CD spectrum of reduced full-length murine PrP(23–231), as reduced murine PrP(121–231) aggregates at any ionic strength at pH 4.0 (Zobeley and Glockshuber, unpublished data). Neither reduced PrP(121–231)-ΔH1 nor reduced H2–H3 showed β-sheet like far-UV-CD spectra comparable to the spectrum of reduced PrP(23–231) (Fig. 4), albeit the molar mean residue ellipticities are significantly less negative compared to the oxidized proteins and are slightly shifted towards lower wavelengths. Overall, the CD spectra of the reduced deletion variants demonstrate that the complete loss of α-helical CD signal observed for reduced, recombinant human PrP(91–231), hamster PrP(90–231) and murine PrP(23–231) must be triggered by the segment comprising α-helix 1 and/or segment 90–120. Our data also indicate that reduced PrP(90–231) and PrP(23–231) adopt a completely different tertiary structure at acid pH that involves the H2–H3 segment, because the α-helical signal is completely missing in the far-UV-CD spectra of reduced PrP(23–231) (Fig. 4).

4. Conclusion

In the present study, we have addressed the question of whether parts of the tertiary structure of PrP^{C} are sufficiently stable to be retained in PrP^{Sc}, the abnormal, oligomeric PrP isoform believed to cause TSEs in mammalians. For this purpose, deletion variants of the folded domain of recombinant PrP were constructed and analyzed for folding and stability. The deletion constructs PrP(121–231)-ΔH1 and H2–H3 both contain the disulfide-linked C-terminal α-helices 2 and 3 of PrP, which form the scaffold of the folded C-terminal PrP domain, PrP(121–231). These α-helices are assumed to represent the most stable part of the structure of PrP(121–231) and to be preserved in models of PrP^{Sc} [12,18]. Although both deletion constructs investigated here essentially retain α-helical structure, they are extremely destabilized compared to PrP(121–231), with free energies of folding close to zero. We conclude

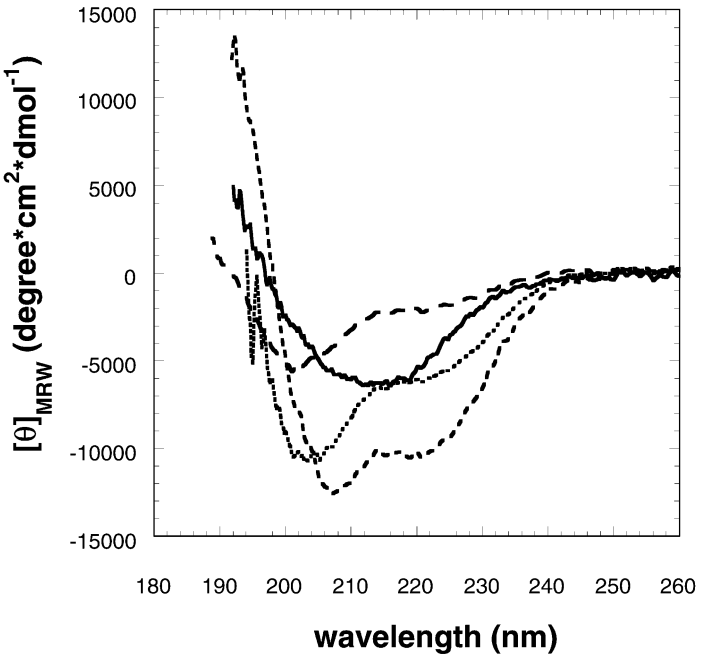

Fig. 4. Far-UV-CD spectra of reduced PrP(23–231) (solid line), reduced PrP(121–231)-ΔH1 (dotted line), reduced H2–H3 (upper dashed line) and oxidized PrP(121–231)-ΔH1 (lower dashed line) at 22 °C and pH 4.0. The spectrum of oxidized H2–H3, which coincides with that of oxidized PrP(121–231)-ΔH1 at pH 4.0 (see Fig. 2b), is not shown for clarity.

from these data that the tertiary structure of segment 170–231 in PrP^{Sc} subunits could well differ from that observed in PrP^{C}. This would be consistent with the fact that the domain PrP(121–231) shows two-state folding behavior [11,48], and is assumed to unfold completely prior to the transition to PrP^{Sc}. Previous hydrogen exchange experiments have demonstrated that only a small, structured nucleus of approximately 10 residues around the disulfide bond is retained in the unfolded state of PrP. Thus if one would assume a tertiary structure context in PrP^{Sc} that destabilizes the helical conformation of segment 170–231, this nucleus might be the only element of PrP^{C} preserved in PrP^{Sc} [11].

The recently solved NMR structures of recombinant human and bovine PrP, and of single amino acid variants of human PrP revealed a striking correlation between local structural differences between PrPs from different species, and the observed species barrier of TSE transmission [5,23,52]. One possible explanation for this correlation would be that the PrP^{C} regions with largest structural differences between species, i.e. α-helix 3 and a segment of irregular secondary structure preceding α-helix 2 [5], are retained in PrP^{Sc} subunits and thereby prevent formation of regular PrP^{Sc} hetero-oligomers. However, the present data would also be consistent with a different model for the species barrier phenomenon in which a host-specific factor (‘protein *X*’) required for PrP^{Sc} propagation, discriminates between PrPs from different species at the level of PrP^{C} [45].

Acknowledgments

This project was supported by the Schweizerisches Bundesamt fuer Bildung und Wissenchaft (grant 97.0578-1) and The Swiss National Science Foundation (grant 438+050285).

References

[1] T. Alper, W.A. Cramp, D.A. Haig, M.C. Clarke, Does the agent of scrapie replicate without nucleic acid?, Nature 214 (1967) 764–766.

[2] T. Alper, The scrapie enigma: insights from radiation experiments. 1993 (classical article), Int. J. Radiat. Biol. 71 (1997) 759–768.
[3] M.A. Baldwin, K.M. Pan, J. Nguyen, et al., Spectroscopic characterization of conformational differences between PrPC and PrPSc: an α-helix to β-sheet transition, Philos. Trans. R. Soc. Lond. B Biol. Sci. 343 (1994) 435–441.
[4] H. Büeler, A. Aguzzi, A. Sailer, et al., Mice devoid of PrP are resistant to scrapie, Cell 73 (1993) 1339–1347.
[5] L. Calzolai, D.A. Lysek, P. Güntert, et al., NMR structures of three single-residue variants of the human prion protein, Proc. Natl. Acad. Sci. USA 97 (2000) 8340–8345.
[6] G.L. Ellmann, Tissue sulfhydryl groups, Arch. Biochem. Biophys. 82 (1959) 70–77.
[7] S.C. Gill, P.H. von Hippel, Calculation protein extinction coefficients from amino acid sequence data, Anal. Biochem. 182 (1989) 319–326.
[8] R. Glockshuber, Folding dynamics and energetics of recombinant prion proteins, Adv. Protein Chem. 57 (2001) 83–105.
[9] S. Hornemann, R. Glockshuber, Autonomous and reversible folding of a soluble amino-terminally truncated segment of the mouse prion protein, J. Mol. Biol. 261 (1996) 614–618.
[10] S. Hornemann, R. Glockshuber, A scrapie-like unfolding intermediate of the prion protein domain PrP(121–231) induced by acidic pH, Proc. Natl. Acad. Sci. USA 95 (1998) 6010–6014.
[11] L.L.P. Hosszu, N.J. Baxter, G.S. Jackson, et al., Structural mobility of the human prion protein probed by backbone hydrogen exchange, Nat. Struct. Biol. 6 (1999) 740–743.
[12] Z. Huang, S.B. Prusiner, F.E. Cohen, Scrapie prions: a three-dimensional model of an infectious fragment, Fold. Des. 1 (1996) 13–19.
[13] G.S. Jackson, L.L. Hosszu, A. Power, et al., Reversible conversion of monomeric human prion protein between native and fibrilogenic conformations, Science 283 (1999) 1935–1937.
[14] T.L. James, H. Liu, N.B. Ulyanov, et al., Solution structure of a 142-residue recombinant prion protein corresponding to the infectious fragment of the scrapie isoform, Proc. Natl. Acad. Sci. USA 94 (1997) 10086–10091.
[15] K. Kellings, N. Meyer, C. Mirenda, S.B. Prusiner, D. Riesner, Analysis of nucleic acids in purified scrapie prion preparations, Arch. Virol. Suppl. 7 (1993) 215–225.
[16] K. Kellings, S.B. Prusiner, D. Riesner, Nucleic acids in prion preparations: unspecific background or essential component?, Philos. Trans. R. Soc. Lond. B Biol. Sci. 343 (1994) 425–430.
[17] R. Koradi, M. Billeter, K. Wüthrich, MOLMOL: a program for display and analysis of macromolecular structures, J. Mol. Graph. 14 (51–55) (1996) 29–32.
[18] C. Korth, B. Stierli, P. Streit, et al., Prion (PrPSc)-specific epitope defined by a monoclonal antibody, Nature 390 (1997) 74–77.
[19] T.A. Kunkel, Rapid and efficient site-specific mutagenesis without phenotypic selection, Proc. Natl. Acad. Sci. USA 82 (1985) 488–492.
[20] T.A. Kunkel, J.D. Roberts, R.A. Zabour, Rapid and efficient site-specific mutagenesis without phenotypic selection, Methods Enzymol. 154 (1987) 367–382.
[21] C.I. Lasmezas, J. Fournier, V. Nouvel, et al., Adaption of the bovine spongiform encephalopathy agent to primates and comparison with Creutzfeldt–Jakob disease: implications for human health, Proc. Natl. Acad. Sci. USA 98 (2001) 4142–4147.
[22] S. Liemann, R. Glockshuber, Influence of amino acid substitutions related to inherited human prion diseases on the thermodynamic stability of the cellular prion protein, Biochemistry 38 (1999) 3258–3267.
[23] F. Lopez Garcia, R. Zahn, R. Riek, K. Wüthrich, NMR structure of the bovine prion protein, Proc. Natl. Acad. Sci. USA 97 (2000) 8334–8339.
[24] N.R. Maiti, W.K. Surewicz, The role of disulfide bridge in the folding and stability of the recombinant human prion protein, J. Biol. Chem. 276 (2001) 2427–2431.
[25] R.K. Meyer, M.P. McKinley, K.A. Bowman, M.B. Braunfeld, R.A. Barry, S.B. Prusiner, Separation and properties of cellular and scrapie prion proteins, Proc. Natl. Acad. Sci. USA 83 (1986) 2310–2314.
[26] I. Mehlhorn, D. Groth, J. Stockel, et al., High-level expression and characterization of a purified 142-residue polypeptide of the prion protein, Biochemistry 35 (1996) 5528–5537.
[27] M. Morillas, D.L. Vanik, W.K. Surewicz, On the mechanism of α-helix to β-sheet transition in the recombinant prion protein, Biochemistry 40 (2001) 6982–6987.
[28] J.K. Myers, C.N. Pace, J.M. Scholtz, Denaturant *m* values and heat capacity changes: relation to changes in accessible surface areas of protein unfolding, Protein Sci. 4 (1995) 2138–2148.
[29] K.M. Pan, M. Baldwin, J. Nguyen, et al., Conversion of α-helices into β-sheets features in the formation of the scrapie prion proteins, Proc. Natl. Acad. Sci. USA 90 (1993) 10962–10966.
[30] S.B. Prusiner, Novel proteinaceous infectious particles cause scrapie, Science 216 (1982) 136–144.
[31] S.B. Prusiner, The prion diseases. Sci. Am. January (1995) 30–37.
[32] S.B. Prusiner, Molecular biology and pathogenesis of prion diseases, Trends Biochem. Sci. 21 (1996) 482–487.
[33] S.B. Prusiner, Prion diseases and the BSE crisis, Science 278 (1997) 245–250.
[34] R. Riek, S. Hornemann, G. Wider, M. Billeter, R. Glockshuber, K. Wüthrich, NMR structure of the mouse prion protein domain PrP(121–231), Nature 382 (1996) 180–182.

[35] R. Riek, S. Hornemann, G. Wider, R. Glockshuber, K. Wüthrich, NMR characterization of the full-length recombinant murine prion protein, mPrP(23–231), FEBS Lett. 413 (1997) 282–288.

[36] M.M. Santoro, D.W. Bolen, Unfolding free energy changes determined by the linear extrapolation method. 1. Unfolding of phenylmethanesulfonyl α-chymotrypsin using different denaturants, Biochemistry 27 (1988) 8063–8068.

[37] H.M. Schätzl, M. da Costa, L. Taylor, F.E. Cohen, S.B. Prusiner, Prion protein gene variation among primates [published erratum appears in J. Mol. Biol. (1997) 265–257.), J. Mol. Biol. 245 (1995) 362–374.

[38] M.R. Scott, R. Will, J. Ironside, et al., Compelling transgenic evidence for transmission of bovine spongiform encephalopathy prions to humans, Proc. Natl. Acad. Sci. USA 96 (1999) 15137–15142.

[39] B.L. Sibanda, T.L. Blundell, J.M. Thornton, Conformation of β-hairpins in protein structures, J. Mol. Biol. 206 (1989) 759–777.

[40] B.L. Sibanda, J.M. Thornton, hairpin families in globular proteins, Nature 316 (1985) 170–174.

[41] N. Stahl, S.B. Prusiner, Prions and prion proteins, FASEB J. 5 (1991) 2799–2807.

[42] N. Stahl, M.A. Baldwin, D.B. Teplow, et al., Structural studies of the scrapie prion protein using mass spectrometry and amino acid sequencing, Biochemistry 32 (1993) 1991–2002.

[43] S. Strobl, P. Mühlhahn, R. Bernstein, et al., Determination of the three-dimensional structure of the bifunctional α-amylase/trypsin inhibitor from Ragi seeds by NMR-spectroscopy, Biochemistry 34 (1995) 8281–8293.

[44] W. Swietnicki, R. Petersen, P. Gambetti, W.K. Surewicz, pH-dependent stability and conformation of the recombinant human prion protein PrP(90–231), J. Biol. Chem. 272 (1997) 27517–27520.

[45] G.C. Telling, M. Scott, J. Mastrianni, et al., Prion propagation in mice expressing human and chimeric PrP transgenes implicates the interaction of cellular PrP with another protein, Cell 83 (1995) 79–90.

[46] J. Vieira, J. Messing, Production of single-stranded plasmid-DNA, Methods Enzymol. 153 (1987) 3–11.

[47] C. Weissmann, The Ninth Data Lecture. Molecular biology of transmissible spongiform encephalopathies, FEBS Lett. 389 (1996) 3–11.

[48] G. Wildegger, S. Liemann, R. Glockshuber, Extremely rapid folding of the C-terminal domain of the prion protein without kinetic intermediates, Nat. Struct. Biol. 6 (1999) 550–553.

[49] F. Wopfner, G. Weidenhofer, R. Schneider, et al., Analysis of 27 mammalian and 9 avian PrPs reveals high conservation of flexible regions of the prion protein, J. Mol. Biol. 289 (1999) 1163–1178.

[50] H. Zhang, J. Stockel, I. Mehlhorn, et al., Physical studies of conformational plasticity in a recombinant prion protein, Biochemistry 36 (1997) 3543–3553.

[51] R. Zahn, C. von Schroetter, K. Wüthrich, Human prion proteins expressed in *Escherichia coli* and purified by high-affinity column refolding, FEBS Lett. 417 (1997) 400–404.

[52] R. Zahn, A. Liu, T. Lührs, et al., NMR solution structure of the human prion protein, Proc. Natl. Acad. Sci. USA 97 (1) (2000) 145–150.